1-1-2008

Self-healing properties of optical Airy beams

John Broky
University of Central Florida

Georgios A. Siviloglou
University of Central Florida

Aristide Dogariu
University of Central Florida

Demetrios N. Christodoulides
University of Central Florida

Self-healing properties of optical Airy beams

John Broky, Georgios A. Siviloglou, Aristide Dogariu, and Demetrios N. Christodoulides

CREOL/College of Optics & Photonics, University of Central Florida, Orlando, FL 32816

Abstract: We investigate both theoretically and experimentally the self-healing properties of accelerating Airy beams. We show that this class of waves tends to reform during propagation in spite of the severity of the imposed perturbations. In all occasions the reconstruction of these beams is interpreted through their internal transverse power flow. The robustness of these optical beams in scattering and turbulent environments is also studied experimentally. Our observations are in excellent agreement with numerical simulations.

OCIS codes: (260.2110) Electromagnetic optics; (350.5500) Propagation; (290.5850)Scattering, particles; (290.7050) Turbid media.

References and links

1. G. A. Siviloglou and D. N. Christodoulides, "Accelerating finite energy Airy beams," Opt. Lett. **32**, 979-981 (2007).
2. G. A. Siviloglou, J. Broky, A. Dogariu, and D. N. Christodoulides, "Observation of accelerating Airy beams," Phys. Rev. Lett. **99**, 213901 (2007).
3. G. A. Siviloglou, J. Broky, A. Dogariu, and D. N. Christodoulides, "Ballistic dynamics of Airy beams," Opt. Lett. **33**, 207-209 (2008).
4. I. M. Besieris and A. M. Shaarawi, "A note on an accelerating finite energy Airy beam," Opt. Lett. **32**, 2447-2249 (2007).
5. M. V. Berry and N. L. Balazs, "Nonspreading wave packets," Am. J. Phys. **47**, 264-267 (1979).
6. K. Dholakia, "Optics: Against the spread of the light," Nature **451**, 413 (2008).
7. M. A. Bandres and J. C. Gutiérrez-Vega, "Airy-Gauss beams and their transformation by paraxial optical systems," Opt. Express **15**, 16719-16728 (2007).
8. H. I. Sztul and R. R. Alfano, "The Poynting vector and angular momentum of Airy beams," Opt. Express **16**, 9411-9416 (2008).
9. M. Asorey, P. Facchi, V. I. Man'ko, G. Marmo, S. Pascazio, and E. C. G. Sudarshan, "Generalized tomographic maps," Phys. Rev. A. **77**, 042115 (2008).
10. A. V. Gorbach and D. V. Skryabin, "Soliton self-frequency shift, non-solitonic radiation and self-induced transparency in air-core fibers," Opt. Express **16**, 4858-4865 (2008).
11. P. Saari, "Laterally accelerating Airy pulses," Opt. Express **16**, 10303-10308 (2008).
12. J. Durnin, J. J. Miceli, and J. H. Eberly, "Diffraction-free beams," Phys. Rev. Lett. **58**, 1499-1501 (1987).
13. D. McGloin and K. Dholakia, "Bessel beams: diffraction in a new light," Contemp. Phys. **46**, 15-28 (2005).
14. R. P. MacDonald, S. A. Boothroyd, T. Okamoto, J. Chrostowski, and B. A. Syrett, "Interboard optical data distribution by Bessel beam shadowing," Opt. Commun. **122**, 169-177 (1996).
15. Z. Bouchal, J. Wagner, and M. Chlup, "Self-reconstruction of a distorted nondiffracting beam," Opt. Commun. **151**, 207-211 (1998).
16. V. Garces-Chavez, D. McGloin, H. Melville,W. Sibbett, and K. Dholakia, "Simultaneous micromanipulation in multiple planes using a self-reconstructing light beam," Nature **419**, 145-147 (2002).
17. O. Vallée and M. Soares, *Airy Functions and Applications to Physics*, (Imperial College Press, London, 2004).
18. L. Allen, M. W. Beijersbergen, R. J. C. Spreeuw, and J. P. Woerdman, "Orbital angular momentum of light and the transformation of Laguerre-Gaussian laser modes," Phys. Rev. A. **45**, 8185-8189 (1992).
19. H.C. van de Hulst, *Light Scattering by Small Particles*, (Dover Publication Inc., New York, 1981).
20. S. Prahl, "Mie Scattering Calculator," (2008). http://omlc.ogi.edu/calc/mie_calc.html
21. J. F. Nye and M. V. Berry, "Dislocations in wave trains," Proc. R. Soc. London Ser. A **336**, 165-190 (1974).
22. A. Dogariu and S. Amarande, "Propagation of partially coherent beams: turbulence-induced degradation," Opt. Lett. **28,** 10-12 (2003).

1. Introduction

Quite recently accelerating Airy beams have been predicted within the framework of optics [1]. As it was demonstrated in this theoretical study [1], this novel class of waves can exhibit two key characteristics: they remain approximately diffraction-free while their intensity

#98252 - $15.00 USD Received 2 Jul 2008; revised 1 Aug 2008; accepted 5 Aug 2008; published 8 Aug 2008

features tend to transversely accelerate (or self-bend) during propagation. This suggestion led to the first experimental realization of optical Airy beams where these intriguing properties were directly observed in one- and two-dimensional configurations [2]. In a subsequent study the ballistic dynamics of Airy beams were also studied experimentally, indicating that these waves can move along parabolic trajectories-akin to those of projectiles under the action of gravity-while their center of gravity follows a straight line [3,4]. We note that these finite-energy beams are mathematically related to the non-spreading Airy wavepackets initially considered by Berry and Balazs within the context of quantum mechanics [5].

These works generated interest in further exploring the nature and peculiarities of Airy beams [6-11]. More specifically Besieris and Shaarawi showed that the centroid of Airy beams varies linearly with range [4]. Bandres and Gutiérrez-Vega studied the propagation of Airy beams in ABCD systems [7] while Sztul and Alfano investigated in detail the evolution of their Poynting vector and angular momentum [8]. The possibility of realizing generalized tomographic maps using Airy waves was suggested by Asorey et al [9]. Spatiotemporal Airy wavepackets can also be encountered in dispersive environments [1,2], and Airy tails can be observed during non-solitonic radiation as indicated by Gorbach and Skryabin [10].

Perhaps one of the most remarkable properties of any diffraction-free beam [12,13] is its very ability to self-reconstruct during propagation [14,15]. This characteristic is of particular importance especially when such waves propagate in inhomogeneous media [16]. The question naturally arises whether Airy beams can self-heal themselves and to what extent? If so, how does this process take place and how is it affected by the beam's acceleration dynamics? For example, can an Airy beam negotiate adverse environments?

In this work we study both theoretically and experimentally the self-healing properties of optical Airy beams. We show that this family of waves exhibits remarkable resilience against perturbations and tends to reform during propagation. In all the examined physical settings the reconstruction of these beams is monitored through their internal transverse power flow. The robustness of these optical beams in adverse environments such as in scattering and turbulent media is also studied experimentally. Our observations are in excellent agreement with numerical simulations. Finally, we have demonstrated that an Airy beam can retain its shape under turbulent conditions as opposed to a Gaussian beam that suffers massive deformations in the same environment.

2. Dynamics of optical Airy beams

To analyze the propagation behavior of optical Airy beams we employ the normalized paraxial equation of diffraction [1-3]:

$$i\frac{\partial\phi}{\partial z}+\frac{1}{2k}\frac{\partial^2\phi}{\partial x^2}+\frac{1}{2k}\frac{\partial^2\phi}{\partial y^2}=0 \tag{1}$$

where ϕ is the electric field envelope and $k=2\pi n/\lambda_0$ is the wavenumber of the optical wave. Following the approach of Ref. [1], the evolution of a two-dimensional finite energy accelerating Airy beam, whose field profile at the origin is given by $\phi(x,y,z=0)=\prod_{m=x,y}Ai(s_m)\exp(a_m s_m)\exp(iv_m s_m)$, can be obtained in closed form:

$$\phi(x,y,z)=\prod_{m=x,y}u_m(s_m,\xi_m) \tag{2a}$$

where

$$\begin{aligned}u_m(s_m,\xi_m)=Ai\left[s_m-(\xi_m/2)^2-v_m\xi_m+ia_m\xi_m\right]\times\exp\left[a_m s_m-\left(a_m\xi_m^2/2\right)-a_m v_m\xi_m\right]\\ \times\exp\left[i\left(-\left(\xi_m^3/12\right)+\left((a_m^2-v_m^2+s_m)\xi_m/2\right)+v_m s_m-(v_m\xi_m^2/2)\right)\right]\ .\end{aligned} \tag{2b}$$

#98252 - $15.00 USD Received 2 Jul 2008; revised 1 Aug 2008; accepted 5 Aug 2008; published 8 Aug 2008

$Ai(s_m)$ denotes the Airy function [17], $s_x = x/x_0$ and $s_y = y/y_0$ represent dimensionless transverse coordinates, with x_0, y_0 being arbitrary transverse scales, and $\xi_x = z/kx_0^2$ and $\xi_y = z/ky_0^2$ are used to normalize the propagation distance z. a_m in the exponential function is a small positive parameter associated with the effective aperture of the system, and v_m is related to the initial launch angle θ_m (or "velocity") of this beam through $\theta_m = v_m/k(x_0, y_0)$ [3]. Figure 1 shows experimental results at $z = 0$ and $z = 20cm$ describing the evolution of a two-dimensional Airy beam when $a_m = 0.08$ $(m = x, y)$, $x_0 \approx 150\mu m$ and $y_0 \approx 77\mu m$. The scaling bar in Fig. 1(a). and in all the figures of this work corresponds to $200\mu m$.

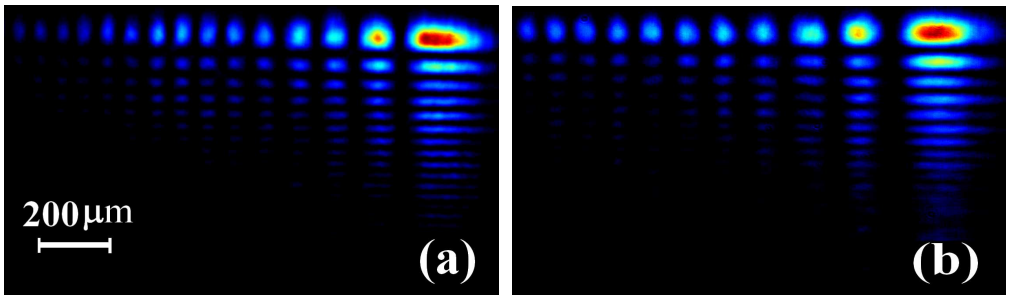

Fig. 1. Intensity cross-sections of an experimentally observed two-dimensional Airy beam with $x_0 = 150\mu m$ and $y_0 = 77\mu m$ and $a = 0.08$ at (a) $z = 0$ and (b) $z = 20cm$.

From Eq. 2(b) one can also directly determine the trajectory of the main (corner) lobe of the Airy beam as a function of distance. This 3D curve is given by:

$$x_d = \frac{1}{4k^2 x_0^3} z^2 + \theta_x z$$
$$y_d = \frac{1}{4k^2 y_0^3} z^2 + \theta_y z \,. \qquad (3)$$

In principle this trajectory can be appropriately tailored through the magnitude and sign of the launch angles θ_m, and the scales x_0, y_0. Clearly, for zero launch angles θ_m and if $x_0 = y_0$, the main lobe of the Airy beam will move on a parabola (projected along the 45° axis in the $x - y$ plane). On the other hand, a "boomerang-like" curve may result if for example the "launch" angles are chosen to have opposite signs, say $\theta_x = -2mrad$ and $\theta_y = 2mrad$ (while $x_0 = y_0 = 77\mu m$), as shown in Fig. 2. What is also very interesting is the fact that these displacements vary quadratically with the wavelength λ_0.

#98252 - $15.00 USD Received 2 Jul 2008; revised 1 Aug 2008; accepted 5 Aug 2008; published 8 Aug 2008

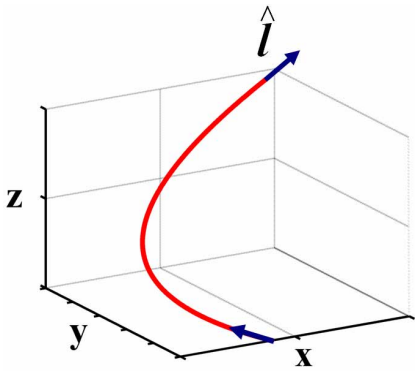

Fig. 2. Motion of the main lobe of a symmetric $(x_0 = y_0 = 77\mu m)$ Airy beam when launched at $\theta_x = -2mrad$ and $\theta_y = 2mrad$.

The self-healing properties of a non-diffracting (ND) field configuration, when it is partially blocked by a finite opaque obstacle at $z = 0$, can be explained from Babinet's principle [15]. If the non-diffracting input field is disturbed by a finite energy perturbation $\varepsilon(x, y)$, i.e. $\phi(x, y, z = 0) = U_{ND}(x, y, z = 0) - \varepsilon(x, y, z = 0)$, then from Eq. (1) one finds that $i\varepsilon_z + (1/2k)\nabla_\perp^2 \varepsilon = 0$. As a result the perturbation ε is expected to rapidly diffract as opposed to the non-diffracting beam that remains invariant during propagation. As a consequence, at large distances $|\phi(x, y, z)|^2 \cong |U_{ND}(x, y, z)|^2$, and hence the ND beam reforms during propagation. This argument holds for all ND fields including the accelerating Airy beam.

Of relevance to our discussion is the Poynting vector $\vec{S}$ associated with Airy optical beams. In the paraxial regime, $\vec{S}$ is given by [18]:

$$\vec{S} = \vec{S}_z + \vec{S}_\perp = \frac{1}{2\eta_0}|\phi|^2 \hat{z} + \frac{i}{4\eta_0 k}\left[\phi \nabla_\perp \phi^* - \phi^* \nabla_\perp \phi\right] \tag{4}$$

where $\eta_0 = \sqrt{\mu_0/\varepsilon_0}$ is the impedance of free space. $\vec{S}_z$ denotes the longitudinal component of the Poynting vector whereas $\vec{S}_\perp$ the transverse. From Eqs. (3, 4) one can directly obtain the direction of the Poynting vector associated with an ideal 2D Airy ($a_m = 0$) beam, as schematically indicated in Fig. 3.

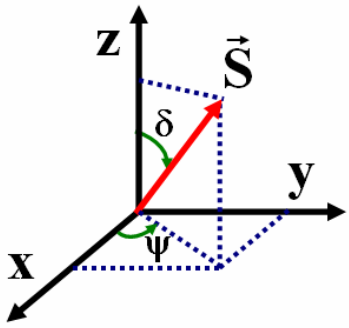

Fig. 3. Schematic representation of the Poynting vector $\vec{S}$ in a Cartesian system of coordinates.

#98252 - $15.00 USD Received 2 Jul 2008; revised 1 Aug 2008; accepted 5 Aug 2008; published 8 Aug 2008

More specifically, the angle ψ the projection of $\vec{S}$ makes with respect to x axis is given by:

$$\tan\psi = \frac{S_y}{S_x} = \frac{\theta_y + \dfrac{z}{2k^2 y_0^3}}{\theta_x + \dfrac{z}{2k^2 x_0^3}}. \qquad (5)$$

On the other hand, the direction of $\vec{S}$ relative to the z axis is given by:

$$\tan\delta = \frac{\sqrt{S_x^2 + S_y^2}}{S_z} = \sqrt{\left(\theta_x + \frac{z}{2k^2 x_0^3}\right)^2 + \left(\theta_y + \frac{z}{2k^2 y_0^3}\right)^2} \quad . \qquad (6)$$

Note that for ideal Airy beams, the Poynting vector $\vec{S}$ is at every point parallel to the unit tangent vector $\hat{l}$ of the trajectory curve of Eq. (3) (see Fig. 2). This statement is also valid for finite energy Airy beams during the quasi-diffraction free stage of propagation. At larger distances however small deviations are expected to occur as shown in Fig. 4 for the 1D case. In addition one can show that the polarization of the beam can evolve in a similar manner.

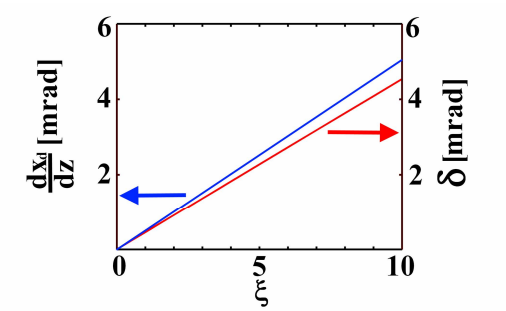

Fig. 4. Direction of the Poynting vector $\vec{S}$ (red line) associated with an one-dimensional finite energy Airy when $a = 0.05$ and $x_0 = 77\mu m$ as a function of distance ξ. The blue line depicts the direction of the tangent unit vector $\hat{l}$ of an ideal Airy beam ($a = 0$ and $x_0 = 77\mu m$).

The reconstruction of an accelerating optical Airy beam will be monitored in our work through the transverse component of the Poynting vector $\vec{S}_\perp$.

3. Experimental Set-up

The experimental set-up used to generate Airy beams is shown in Fig. 5(a). As in Refs. [2,3], the Airy wavefront $Ai(x/x_0)\exp(ax/x_0)Ai(y/y_0)\exp(ay/y_0)$ is produced by Fourier transforming a broad Gaussian beam when a 2D cubic phase modulation is imposed. A linearly polarized Gaussian beam from an Argon-ion laser at $488\,nm$ is collimated using a beam expander to a beam width of $6.7\,mm$. The cubic phase (Fig. 5(b)) was introduced using a computer controlled spatial light modulator (SLM). A spherical lens L with a focal length $f = 1\,m$ was placed at a distance f in front of the SLM phase array in order to generate the finite energy two-dimensional Airy wavepacket. The exponentially truncated Airy function ($x_0 = y_0 \cong 77\mu m$, $a = 0.08$) is Fourier generated at a distance f after the lens (Fig. 5(c)). The propagation dynamics of these beams can then be recorded, as a function of

#98252 - $15.00 USD Received 2 Jul 2008; revised 1 Aug 2008; accepted 5 Aug 2008; published 8 Aug 2008

propagation distance, by translating the imaging apparatus. In order to block the Airy pattern in a controlled manner a rectangular opaque obstacle was inserted at this point using a micro-positioner.

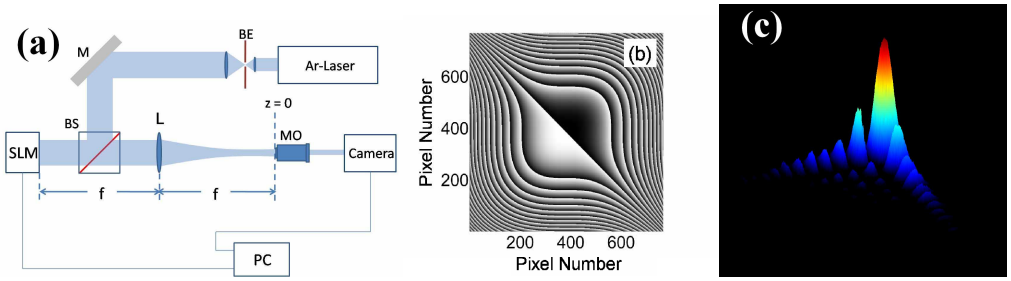

Fig. 5. (a). Experimental set-up, (b). Two-dimensional cubic phase mask, and (c). experimentally observed Airy beam.

4. Self-healing properties of Airy beams

In order to demonstrate the self-healing properties of Airy beams (after they have been perturbed) we monitor their self-reconstruction during propagation. In all cases we block a portion of its initial intensity profile. The most prominent intensity characteristic of an Airy beam happens to be its main corner lobe (as seen in Fig. 5(c)) which contains a large percentage of the beam's total power (in our case almost 40%). In a first experiment, an opaque rectangular obstacle was employed to obstruct the corner lobe of the Airy pattern. The resulting intensity distribution is shown in Fig. 6(a) where the FWHM of the blocked lobe feature was approximately $130\mu m$ corresponding to $x_0 = y_0 \approx 77\mu m$ and $a = 0.08$. Figure 6(b) depicts the reformation of this Airy beam after a distance of $z = 11cm$. The self-healing of this beam is apparent. The main lobe is reborn at the corner and persists undistorted up to a distance of $30cm$ (Fig. 6(c)). In our set up, this latter distance ($30cm$) corresponds approximately to four diffraction lengths of the corner lobe. Our experimental observations are in excellent agreement with numerical results presented in Figs. 6(d)-6(f) for the same propagation distances.

#98252 - $15.00 USD Received 2 Jul 2008; revised 1 Aug 2008; accepted 5 Aug 2008; published 8 Aug 2008

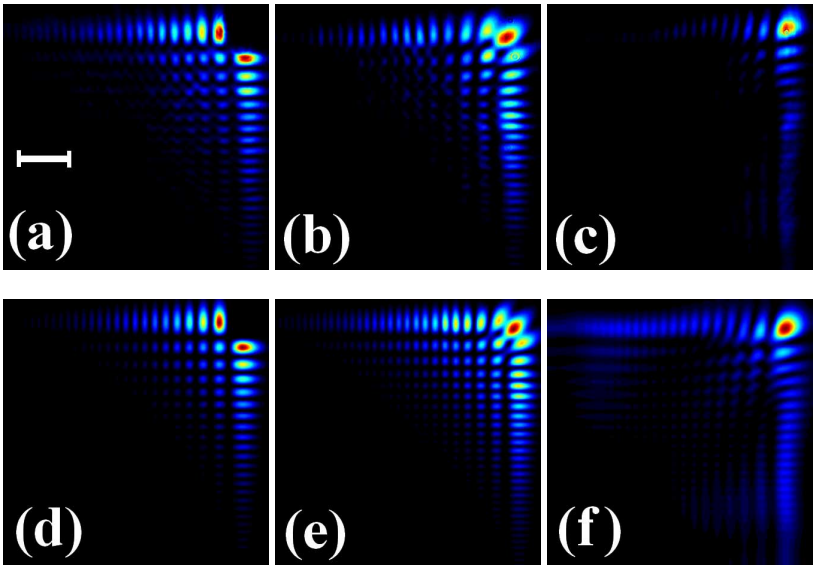

Fig. 6. Self-healing of an Airy beam when its main lobe is blocked. Observed intensity profile at (a) the input $z = 0$, (b) $z = 11cm$, and (c) $z = 30cm$. The corresponding numerical simulations are shown in (d-f).

We note that had the main lobe been launched in isolation it would have experienced a 5-fold increase in the beam width over the same propagation distance, while the peak intensity would have dropped to 5% of its initial value. We have carried out this experiment for comparison purposes. Figure 7(a) shows this main lobe at $z = 0cm$ and after $z = 30cm$ (Fig 7(b)). The corresponding numerical simulations are shown in Figs. 7(c) and 7(d). This is another manifestation of the non-diffracting nature of Airy beams.

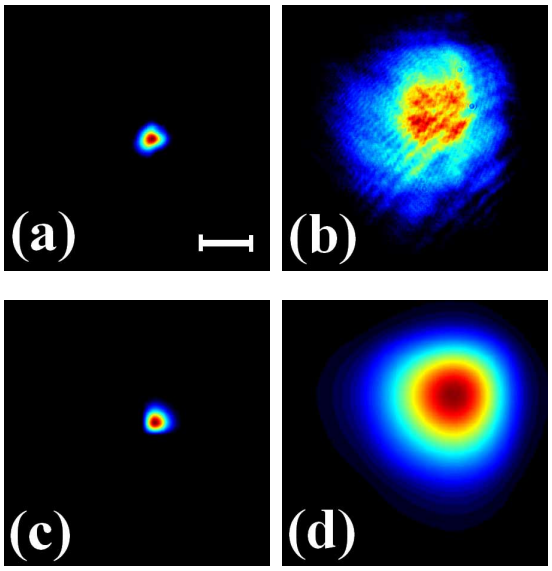

Fig. 7. (a). Main lobe in isolation is observed at $z = 0$, (b) and after diffraction at $z = 30cm$. (c), (d) Corresponding intensity profiles as obtained from theory.

#98252 - $15.00 USD Received 2 Jul 2008; revised 1 Aug 2008; accepted 5 Aug 2008; published 8 Aug 2008

In order to understand this self-healing process it is important to study the internal transverse power flow $\vec{S}_\perp$ within the perturbed Airy beam. To do so we use the result of Eq. (4). Figure 8(a) depicts the transverse flow within the Airy beam at $z = 1cm$ when the main lobe has been removed. Evidently the power flows from the side lobes towards the corner in order to facilitate self-healing. On the other hand, once reconstruction has been reached (at $z = 11cm$), then the internal power density around the newly-formed main lobe flows along the 45° axis in the $x - y$ plane (for $x_0 = y_0$) in order to enable the acceleration dynamics of the Airy beam (Fig. 8(b)).

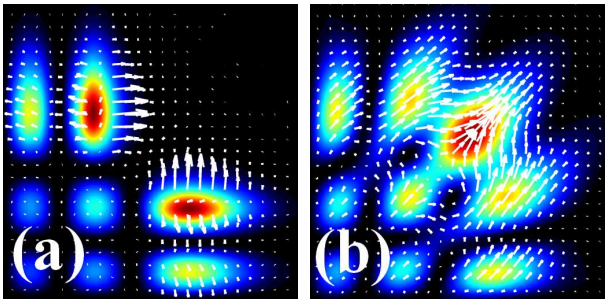

Fig. 8. Calculated transverse power flow $\vec{S}_\perp$ at (a) $z = 1cm$, and (b) $z = 11cm$.

So far we have experimentally demonstrated that an Airy beam can reconstruct itself when its main lobe has been blocked. Of interest will be to examine whether the beam could self-heal even after more severe perturbations. In a second set of experiments we have totally blocked all the internal structure (lobes) of the Airy pattern (Fig. 9(a)). Remarkably after $z = 16cm$ of propagation the beam self-heals and reconstructs in detail its fine intensity structure as depicted in Fig. 9(b). Figures 9(c) and 9(d) show the corresponding calculated intensity profiles for these same distances.

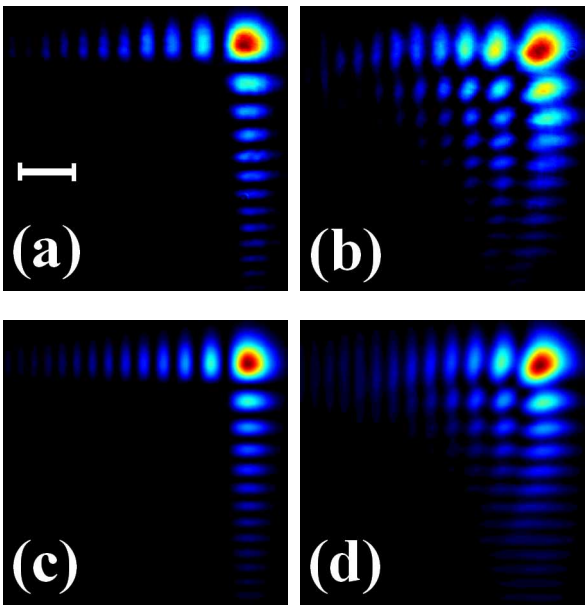

Fig. 9. Self-healing of an Airy beam when all the internal lobes are blocked. Observed intensity profiles at (a) the input $z = 0$ and (b) $z = 16cm$. The corresponding numerical simulations are shown in (c) and (d).

#98252 - $15.00 USD Received 2 Jul 2008; revised 1 Aug 2008; accepted 5 Aug 2008; published 8 Aug 2008

The internal power flow during this latter self-healing process is shown in Fig. 10. At $z = 1cm$, the Poynting vector provides energy towards the blocked region for rebirth to occur while on the main lobe is directed along 45° in the $x - y$ plane in order to enable the self-bending of the Airy beam.

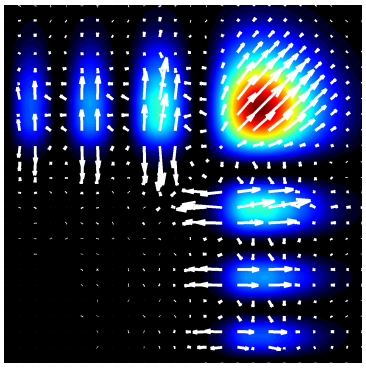

Fig. 10. Transverse power flow $\vec{S}_\perp$ revealing the self-healing mechanism at $z = 1cm$.

Another possibility is to block a 3x3 lobe portion of the Airy beam around its corner as shown in Fig. 11(a) using a metallic obstacle. In this case the beam reforms at $z = 24cm$ (Fig. 11(b)). Compared to the other two cases, this self-healing distance is somewhat longer since the perturbation is now more severe (given the ratio of the power blocked over the incident power). Figures 11(c) and 11(d) show the corresponding simulated patterns while Fig. 11(e) depicts the transverse power flow at $z = 1cm$.

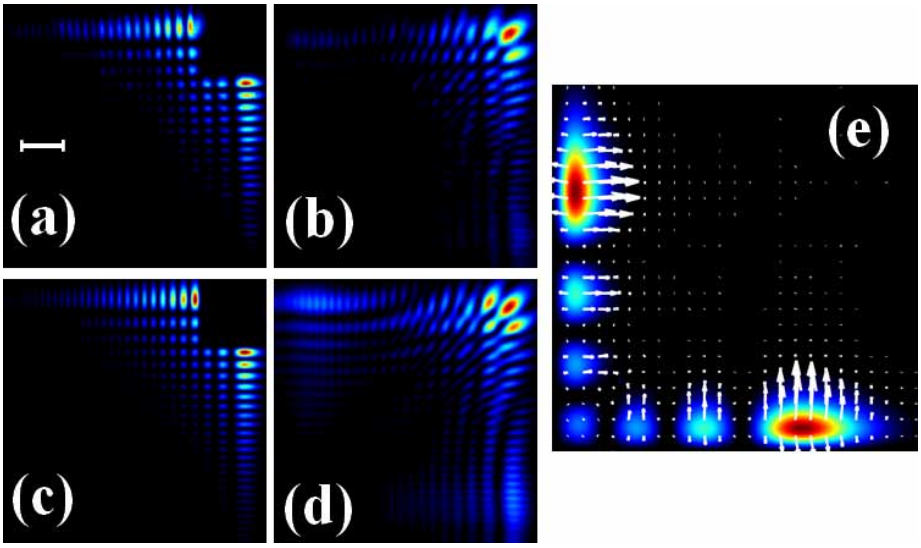

Fig. 11. Self-healing of an Airy beam when a region of 9 lobes is blocked. Observed intensity profiles at (a) the input $z = 0$ and (b) $z = 24cm$. The corresponding numerical simulations are shown in (c) and (d). Calculated transverse power flow $\vec{S}_\perp$ at (e) $z = 1cm$.

Finally we present experimental evidence of Airy beam reconstruction when a non symmetric obstruction is used. This asymmetric perturbation was carried out by blocking the first three lobes of an Airy wavepacket along the y axis as shown in Fig. 12(a). Interestingly,

#98252 - $15.00 USD Received 2 Jul 2008; revised 1 Aug 2008; accepted 5 Aug 2008; published 8 Aug 2008

in this physical setting, the beam not only self-heals itself after $z = 18cm$ but also the initially blocked part is reborn even brighter when compared to its surroundings (Fig. 12(b)). This is a clear manifestation of the non-diffracting character of the Airy beam. The corresponding numerical results (Figs. 12(c) and 12(d)) are in excellent agreement with the experiments.

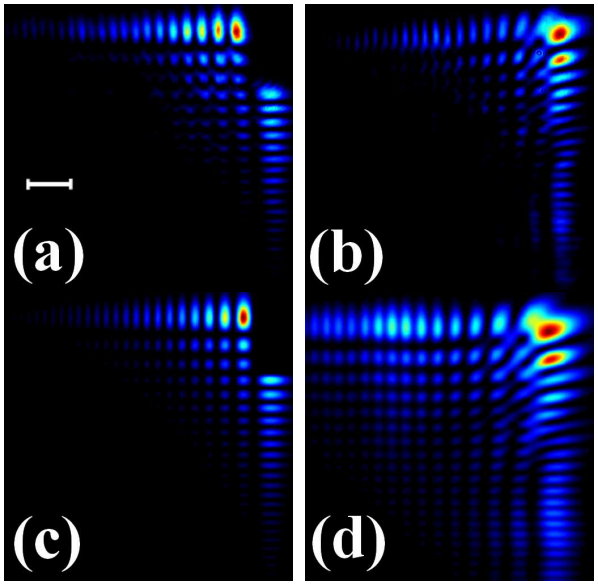

Fig. 12. Self-healing of an Airy beam when 3 lobes along y axis are blocked. Observed intensity cross-sections at (a) the input $z = 0$ and (b) $z = 18cm$. The corresponding numerical simulations are shown in (c) and (d).

5. Propagation of Airy beams in adverse environments

In the previous section we have demonstrated that optical Airy beams are remarkably resilient to amplitude deformations when propagating in free space. The question is: are such self-healing Airy wavepackets also robust in adverse environments? To address this question we have experimentally studied the propagation of Airy beams in scattering and turbulent media.

5.1 Airy beams in scattering media

In order to study the self-healing dynamics of Airy beams in scattering media we have again blocked their main corner lobe (Fig. 13(a)). To do so we have prepared two different samples of silica microspheres ($n = 1.45$) suspended in pure water($n = 1.33$). The size of the dielectric micro-particles was $0.5\mu m$ and $1.5\mu m$ in diameter and thus light scattering was predominantly of the Mie type [19]. Both suspensions were 0.2% in weight concentration while the volume filling factor was 0.1% (the specific gravity of the silica particles is $\rho_{SiO_2} = 2$). We have ultrasonicated the prepared mixtures for one hour, to make sure that the silica particles were mono-dispersedly suspended in water. The scattering cross-section of the microspheres is estimated to be $0.055\mu m^2$ and $3.76\mu m^2$ [20] for the small and large particles respectively. These values lead to significant light scattering, enough to give a granular appearance when the beam propagates $5cm$ in the water-silica mixture (diameter of $0.5\mu m$) (Fig. 13(b)). A longer ($10cm$) cell was used to observe the complete reformation of the Airy pattern in the same scattering media. Figure 13(c) depicts the self-healing of an Airy beam after propagating $10cm$ in the same environment. Besides the anticipated drop in the beam intensity due to Mie scattering, the beam still exhibits in every respect its characteristic pattern.

#98252 - $15.00 USD Received 2 Jul 2008; revised 1 Aug 2008; accepted 5 Aug 2008; published 8 Aug 2008

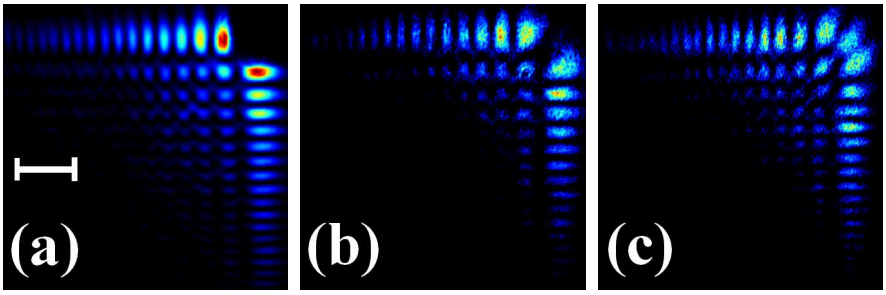

Fig. 13. Self-healing of an Airy beam when propagating in a suspension of $0.5\mu m$ silica micro-spheres in pure water. Observed intensity profiles at (a) the input $z = 0$, (b) $z = 5cm$, and (c) $z = 10cm$.

To complete our observations we have repeated the same experiment with $1.5\mu m$ microspheres having a much larger scattering cross-section and hence more pronounced scattering effects. The self-reconstructed beam at the end of a $10cm$ glass cell is depicted in Fig. 14.

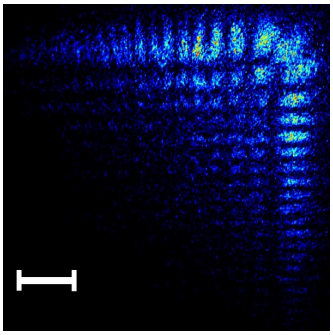

Fig. 14. Self-healing of an Airy beam in a suspension of $1.5\mu m$ silica micro-spheres in pure water after a propagation distance of $z = 10cm$.

5.2 Airy beams in turbulent media

Finally, we have studied the effect of turbulence on an Airy beam. The turbulent environment was realized over a heated rough accordion-shaped aluminum foil above which violent heat convection air currents were generated. The turbulence was controlled by adjusting the temperature of the hotplate around 300 degrees Fahrenheit. The Airy beam was then passed right above the aluminum foil up to a distance of $8cm$. In all our experiments the resilience of the Airy beam (without any initial amplitude distortions) against turbulence was remarkable (Fig. 15(a) and the associated video file). To some extent this robustness can be qualitatively understood if one considers the phase structure of the beam: alternations in phase between 0's and π's result in zero-intensity regions and these singularities can be in turn extremely stable [21,22]. For comparison purposes we turned off the cubic phase from the SLM, thus producing a comparable Gaussian beam. This diffracting Gaussian beam was then passed through the same turbulent system. Unlike the Airy beam, the Gaussian beam suffered massive distortions as it is evident from Fig. 15(b) and the associated video file. Clearly the Gaussian beam is heavily deformed (shape distortion and continuous "center of mass" hopping) and it exhibits a rather involved phase structure.

#98252 - $15.00 USD Received 2 Jul 2008; revised 1 Aug 2008; accepted 5 Aug 2008; published 8 Aug 2008

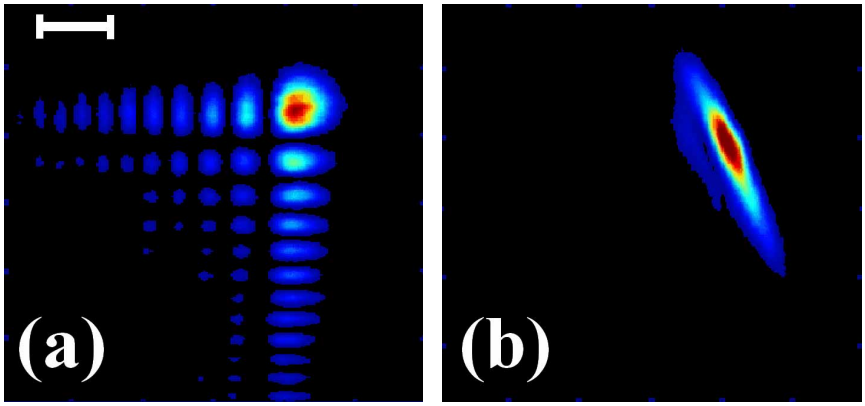

Fig. 15. Propagation in a turbulent medium of (a) (Media 1) an optical Airy beam and (b) (Media 2) a comparable Gaussian beam.

6. Conclusions

In this work we have demonstrated both theoretically and experimentally the self-healing properties of optical Airy beams. By monitoring their internal transverse power flow we have provided insight concerning the self-healing mechanism of Airy beams. We have also experimentally shown that these optical beams can also be robust in adverse environments such as in scattering and turbulent media. Our observations are in excellent agreement with numerical simulations. Finally, we have demonstrated that an Airy beam can retain its shape and structure under turbulent conditions as opposed to a comparable Gaussian beam that suffers from massive deformations. We believe that the robust nature of Airy beams may have important implications in other areas. These may include atmospheric propagation of non-diffracting Airy beams as well as microscopy applications for biological tissues.

Acknowledgment

The authors wish to thank Lockheed Martin Corporation for partially funding this research project.

#98252 - $15.00 USD Received 2 Jul 2008; revised 1 Aug 2008; accepted 5 Aug 2008; published 8 Aug 2008